

22. Fang, J., Wang, X. and Lin, T., Electrical power generator from randomly oriented electrospun poly(vinylidene fluoride) nanofibremembranes. *J. Mater. Chem.*, 2011, **21**(30), 1088–1099.
23. Bauer, S., Gerhard-Mulhaupt, R. and Sessler, G. M., Ferroelectrets: soft electroactive foams for transducers. *Phys. Today*, 2004, **57**, 37–46.
24. Ramaratnam, A. and Jalili, N., Reinforcement of piezoelectric polymers with carbon nanotubes: pathway to next-generation sensors. *J. Intell. Mater. Syst. Struct.*, 2006, **17**, 199–208.
25. Furukawa, T., Lovinger, A. J., Davis, G. T. and Broadhurst, M. G., Dielectric hysteresis and nonlinearity in a 52/48 molcopolymer of vinylidene fluoride and trifluoroethylene. *J. Macromol.*, 1983, **16**(12), 1885–1890.
26. Jin, K. K. and Ling, H. S., An infra-red spectroscopic study of structural reorganization of a uniaxially drawn VDF/TrFE copolymer in an electric field. *J. Macromol.*, 1994, **35**(17), 3612–3618.
27. Xu, H., Cheng, Z. Y., Olson, D., Mai, T., Zhang, Q. M. and Kavarnos, G., Ferroelectric and electromechanical properties of poly(vinylidene-fluoride-trifluoroethylene-chlorotrifluoroethylene) terpolymer. *J. Appl. Phys.*, 2001, **78**(16), 2360–2362.
28. Jin, K. K. and Thein, K., Spinodal phase separation and isothermal crystallization behavior in blends of VDF/TrFE(75/25) copolymer and poly(1,4-butylene adipate) (I). *Fibers Polym.*, 2003, **4**(4), 188–194.
29. Nazir, N. A., Kim, N., Iglesias, W. G., Jakli, A. and Kyu, T., Conductive behavior in relation to domain morphology and phase diagram of Nafion/poly(vinylidene-co-trifluoroethylene) blends. *Polymer*, 2012, **53**, 196–212.
30. Li, B., Xu, C., Zheng, J. and Xu, C., Sensitivity of pressure sensors enhanced by doping silver nanowires. *Sensors*, 2014, **14**(6), 9889–9899.
31. Roh, Y., Varadan, V. V. and Varadan, V. K., Characterization of all the elastic, dielectric, and piezoelectric constants of uniaxially oriented poled PVDF films. *IEEE Trans. Ultrason., Ferroelectr. Freq. Control*, 2002, **49**, 836–847.
32. Sharma, T., Je, S., Gill, B. and Zhang, J. X. J., Patterning piezoelectric thin film PVDF-TrFE based pressure sensor for catheter application. *Sens. Actuat. A*, 2012, **177**, 87–92.
33. Koga, K. and Ohigashi, H., Piezoelectricity and related properties of vinylidene fluoride and trifluoroethylene copolymers. *J. Appl. Phys.*, 1986, **59**(6), 2142–2150.
34. Higashihata, Y., Sako, J. and Yagi, T., Dynamics of ferroelectric phase transition in vinylidene fluoride/trifluoroethylene (VF2/F3E) copolymers. I. Acoustic study. *J. Ferroelectr.*, 1981, **90**(11), 6730–6739.
35. Graz, I. *et al.*, Flexible active-matrix cells with selectively poled bifunctional polymer–ceramic nanocomposite for pressure and temperature sensing skin. *J. Appl. Phys.*, 2009, **106**, 034–503.
36. Dodds, J. S., Meyers, F. N. and Loh, K. J., Piezoelectric characterization of PVDF-TrFE thin films enhanced with ZnO nanoparticles. *IEEE Sens. J.*, 2012, **12**, 1889–1890.
37. Donelan, J. M. *et al.*, Biomechanical energy harvesting: generating electricity during walking with minimal user effort. *J. Sci.*, 2008, **319**(58), 807–810.
38. Cheng, Z. Y., Bharti, V., Xu, T. B., Haisheng, Xu, Mai, T. and Zhang, Q. M., Electrostrictive poly(vinylidene fluoride-trifluoroethylene) copolymers. *Sens. Actuat. A*, 2001, **90**, 138–147.
39. Ramadan, K. S., Sameoto, D. and Evoy, S., A review of piezoelectric polymers as functional materials for electromechanical transducers. *Smart Mater. Struct.*, 2014, **23**, 26–32.
40. Kibria, F. and Patra, S. N., Fabrication of fiber aided nano device for minimally invasive photonics based sub-micron level lesion detection and interventional treatment. *IJREAM*, 2018, **4**(8), 478–484.
41. Park, T., Kim, B., Kim, Y. and Kim, E., Highly conductive PEDOT electrodes for harvesting dynamic energy through piezoelectric conversion. *J. Mater. Chem.*, 2014, 232–241; doi.org/10.1039/c3ta14726f.
42. Toda, M. and Thompson, M. L., Contact-type vibration sensors using curved clamped PVDF film. *IEEE Sens.*, 2006, **6**(5), 1170–1177.

ACKNOWLEDGMENTS. We thank the staff of the ONPDL Lab, Department of Physics, Jadavpur University for technical support. The work was funded by the Departmental Internal Grand Fund for Research of Excellence under Jadavpur University. Permission to collect samples for experimental work was undertaken by the central facilities under Jadavpur University, Kolkata.

Received 24 August 2019; revised accepted 8 January 2020

doi: 10.18520/cs/v119/i5/841-849

## New record of marine red algal species *Grateloupia orientalis* Showe M. Lin & H.Y. Liang and *G. catenata* Yendo (Halymeniaceae, Rhodophyta) from the east coast of India

P. Chellamanimegalai, Annam Pavan-Kumar, Amjad K. Balange, A. Dwivedi and Geetanjali Deshmukhe\*

ICAR-Central Institute of Fisheries Education, Panch Marg, Off Yari Road, Versova, Andheri West, Mumbai 400 061, India

The present study reports the new record of two *Grateloupia* species (Halymeniales, Rhodophyta) namely *Grateloupia orientalis* Showe M. Lin & H.Y. Liang and *G. catenata* Yendo from the coast of Visakhapatnam in Andhra Pradesh, and Tiruchendur in Tamil Nadu, India respectively. Morphological and anatomical studies showed that these differed from the earlier recorded *Grateloupia* species, viz. *G. indica*, *G. filicina* and *G. lithophila*. The descriptive statistics and MDS analysis revealed that these two species differed from the earlier recorded *Grateloupia* sp. The taxonomic evaluation of these two *Grateloupia* species based on chloroplast-encoded *rbcl* gene revealed that they are closely related, sharing few traits between them.

**Keywords:** Coastal regions, descriptive statistics, invasive species, marine red algae, taxonomic evaluation.

THE Rhodophycean algae *Grateloupia* (C. Agardh 1822) is one of the largest genera of family Halymeniaceae with

\*For correspondence. (e-mail: dgeetanjali@cife.edu.in)

more than 90 valid species<sup>1</sup>. The species are native to the West Pacific Ocean and have been introduced to different countries through shipping activity<sup>2,3</sup>. *Grateloupia turu-turu* is one of the species being distributed globally, which is found to be invasive in many countries like Western Europe, North America, and Tasmania<sup>4</sup>. Up till now, six species of *Grateloupia* have been reported from India<sup>5</sup>. Species of family Halymeniaceae can be discriminated by external morphology (thickness of thallus, branching pattern) and internal anatomical structures<sup>6</sup> (reproductive structure, shape, size of the cortex, medullary cell layers, cortex thickness). The genus *Grateloupia* is characterized by compressed to foliose, linear to lanceolate, rarely unbranched, usually branched proliferous thallus, having superficial spermatangia in nemathecium sori, two-celled carpogonia and cruciate tetrasporangia in cortical layer<sup>7</sup>. Nevertheless, several species of the genus share similar morphological characteristics, often leading to misidentification of the species<sup>8</sup>. Molecular markers have been successfully used to resolve the taxonomic ambiguity of marine algae<sup>9-14</sup>.

The present study was carried out to characterize the species of *Grateloupia* from the east coast of India using morphology, anatomy and chloroplast encoded *rbcL* gene. The study reports a new record of *G. orientalis* and *G. catenata* from the Indian coast.

Samples of *G. orientalis* ( $n = 30$ ) were collected from rocky intertidal coast of Visakhapatnam, Andhra Pradesh (17°49'N, 83°24'E) on 5 March 2018, and *G. catenata* ( $n = 30$ ) were obtained from the sandy-cum-rocky intertidal area of Tiruchendur coast, Tuticorin district, Tamil Nadu (8°29'N, 78°07'E) on 4 December 2017. We could not identify any *Grateloupia* species from the Chennai coast. The collected samples were preserved in the form of herbaria for further identification. The herbarium sheets were labelled with collection details and deposited in the Algal Laboratory, FRPHM Division, ICAR-Central Institute of Fisheries Education, Mumbai.

A total of nine morphometric characters, namely height of primary axes (HOPA), width of primary axes (WOPA), length of branch (LOB), width of branch (WOB), length of branchlet (LOBt), width of branchlet (WOBt), diameter of the rhizoid disk (DORD), apical width (AW) and thickness (TK) were measured for all samples of both the species using a digital Vernier caliper. Three meristic traits, viz. number of primary axes (NOPA), number of branches (NOB), and number of branchlets (NOBt) were counted for the species. Descriptive statistics and correlation matrix analysis was performed using SPSS software package version 16 (IBM). To delineate the species using morphological variables, principal component analysis (PCA), multi-dimensional scaling analysis and multivariate test – hierarchical clustering were carried out using PRIMER v 6 (Plymouth Marine Laboratory, United Kingdom). In addition, morphological data of *G. orientalis* and *G. catenata* were

compared with *G. filicina*, *G. lithophila* and *G. indica* to determine the taxonomic differences.

Anatomical evaluation was carried out by a hand-made cross-section as well as the standard histology procedure. The slides were observed under a microscope (OLYMPUS FSX 100), for further characterization of the species.

Total genomic DNA was isolated from fronds of *G. orientalis* ( $n = 3$ ) and *G. catenata* ( $n = 4$ ) by the standard CTAB method, with some modifications<sup>9</sup>. Chloroplast *rbcL* gene (790 bp) was amplified using primers GFFW1: 5'-CCACAACCAGGAGTTGATCC-3' and GFRE1: 5'-ACCATGGCTCTTTTGACGAG-3'. PCR amplification was carried out in a reaction mixture of 25 µl containing 100 ng template DNA sample, 10 pmol of each primer and 1X PCR master mix (ThermoFisher Scientific, USA). The thermal regime for PCR was programmed as initial denaturation at 94°C for 2 min, followed by denaturation at 94°C for 45 sec annealing at 57°C for 30 sec and extension at 72°C for 90 sec for 35 cycles with a final extension at 72°C for 8 min. The amplified product was purified and sequenced in both directions using PCR primers. The quality of the sequence was verified using FinchTv software and the ORF was predicted using the NCBI ORF tool. The sequences were subjected to similarity analysis with the NCBI GenBank database using the BLAST tool. The genetic distance values were estimated and a neighbour-joining (NJ) tree was constructed using MEGA7.0.

*G. orientalis* Showe M. Lin & H.Y. Liang 2008.

Type locality: Linyuan, southwestern Taiwan (22°27'N, 120°27'E) (ref. 10).

Distribution: Asia: Taiwan<sup>10</sup>.

Figure 1 shows the vegetative morphological characteristics of *G. orientalis*. Bushy and cylindrical thallus of *G. orientalis* comprised of many primary axes that arise from a common holdfast, up to 88 mm high, light green to brownish in colour, mucilaginous to cartilaginous in texture, strong discoid holdfast, branches terete to slightly compressed; less number of branches without branchlets and reproductive structure; main axes up to 2–3 mm width at an earlier state, developing stages of thallus contained oppositely or alternately arranged branches, sometimes bearing irregularly pinnate branchlets (Figure 1 a and b). Medullary cells are densely arranged near the cortical layer and become less dense in the middle of the thallus, ovoid in shape, hollow in structure (Figure 1 c and d). Cortex composed of 5–6 cells, inner cortical cells oblong to irregular in shape and loosely arranged; outer cortical cells compact (Figure 1 e). Diploization of auxiliary cells enhances the development of two branches of ampullae filaments from the inner cortex as secondary medullary filaments that were observed in the thallus of *G. orientalis* at the maturing stage (Figure 1 f).

*G. catenata* Yendo 1920

Type locality: Japan<sup>11</sup>.

Distribution: Asia: China, Japan and Korea.

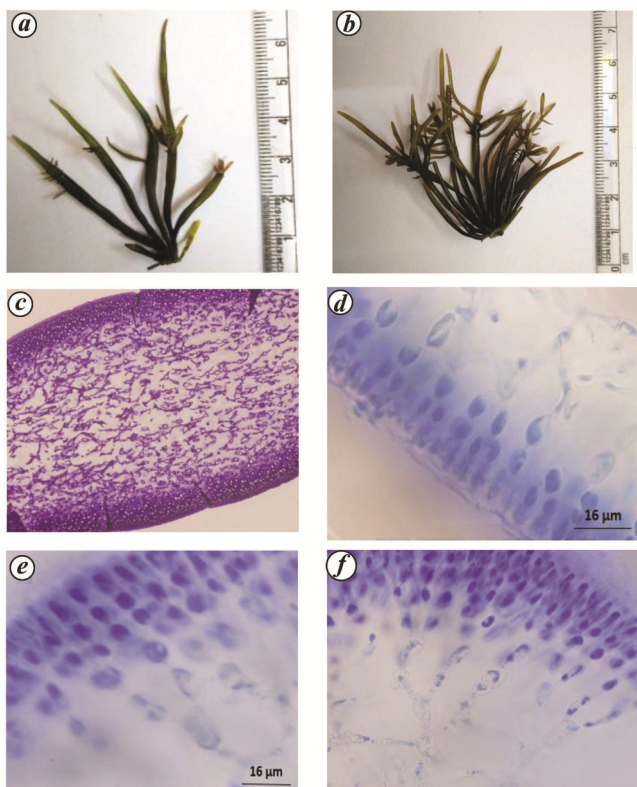
Figure 2 shows the taxonomic characteristics of *G. catenata*. Linear lanceolate and a clump of main axis raised from a large disc of the holdfast, tapering towards the apex, height up to 90 mm; light green to dark green in colour, slippery in texture and highly gelatinous in structure; terete to compressed thallus with thickness up to 1.1 mm; proliferation originates from the anterior tip of branches or throughout the thallus (Figure 2 a and b). Medullary filaments are hollow in nature and oblong in shape, arranged densely near the cortex (Figure 2 c); the cortex layer consists of 5–8 cells, inner cortical cells are irregular and loosely arranged; outer cortical cells are ellipsoidal to sub-spherical, compact and in anti-clinical rows (Figure 2 d). *G. orientalis* and *G. catenata* displayed many morphological similarities such as large holdfast, an assemblage of primary axes making a thallus bushy, gelatinous to cartilaginous in texture, and slippery in nature. According to an earlier study, *G. tenuis*, *G. catenata*, *G. ramosissima*, *G. orientalis* and *G. filiformis* fall under the same subclade of the phylogenetic tree. *G. tenuis* has a slippery and cartilaginous texture, which is different from the mucilaginous and hard texture of

*G. filicina*<sup>12</sup>. The anatomical features (auxiliary cell ampullae, number, and structure of cortical and medullary cells) play a prominent role in distinguishing both species. The hollow structure of the medullary layer was the only similarity between the two species.

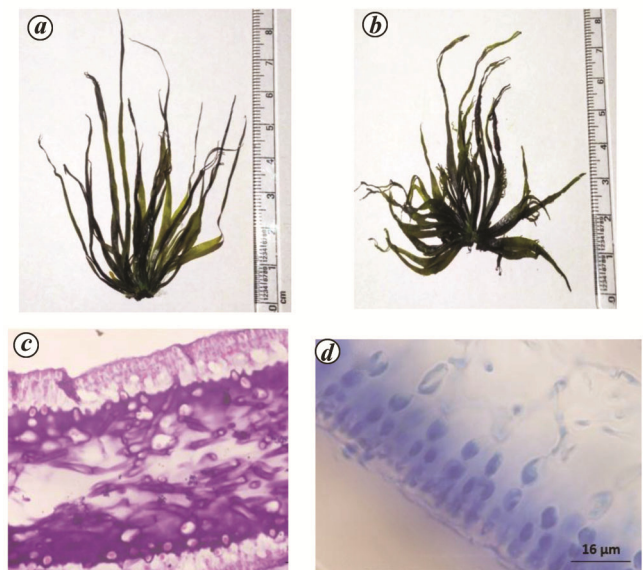
As the samples were not mature, the reproductive structures could not be studied for *G. orientalis* specimens. However, early-stage development of ampullary filament with a continuation of inner cortical cells was observed in *G. orientalis*. Two branches of ampullary filaments formed from an inner cortex as secondary medullary filaments after diploidization of auxiliary cells. This is a unique characteristic of *G. orientalis*. These diverse types of auxiliary cell ampullae have played a vital role in the recognition of *G. orientalis* and *G. taiwanensis*<sup>10</sup>. *G. catenata* lacks ampullary filaments in its inner cortical cell layer, which consists of several minute proliferations throughout the thallus as an external reproductive structure. However, no reproductive structures were observed in the anatomy of *G. catenata*.

Table 1 provides the descriptive statistics of *G. orientalis* and *G. catenata*. The species showed significant difference in length and width of primary axes, presence of branchlets, diameter of rhizoid disk, apical width, thickness and the number of branches on the main axis characters ( $P < 0.5$ ). Branchlets were absent in *G. orientalis*. No significant difference was observed in length and width of the branches, and the number of primary axes (Table 1).

The correlation matrix of morphological characters showed ‘thickness of thallus’ as the most important parameter which is negatively correlated with other



**Figure 1.** Morphology and vegetative anatomy of *Grateloupia orientalis*. a, Young thallus of *G. orientalis*. b, Development of oppositely arranged branches. c, Hollow nature (LS). d, Cortical cells (LS). e, Cortical cells (TS). f, Early development stage of ampullary filament with continuation of inner cortical cells.



**Figure 2.** Morphology and vegetative anatomy of *G. catenata*. a, Young thallus of *G. catenata*. b, Development of proliferation on branches. c, TS of cortical cells. d, LS of cortical cells.

## RESEARCH COMMUNICATIONS

morphological parameters such as length and width of the primary axis, width of branches, length of branchlets, apical width and number of branchlets. Similarly, the number of primary axes and number of branches showed an inverse relationship with length of primary axis, width of primary axis, length of branches, width of branches and number of branchlets (Table 2).

Hierarchical cluster analysis showed *G. orientalis* and *G. catenata* under one subclade that is distant from its

**Table 1.** Descriptive statistics of *Grateloupia orientalis* and *Grateloupia catenata*

Variables (mm)	<i>G. orientalis</i>	<i>G. catenata</i>
HOPA	38.70 ± 2.48 <sup>a</sup>	67.21 ± 3.91 <sup>b</sup>
WOPA	1.34 ± 0.09 <sup>a</sup>	2.63 ± 0.19 <sup>b</sup>
LOB	4.97 ± 0.79 <sup>a</sup>	5.52 ± 2.24 <sup>a</sup>
WOB	0.47 ± 0.06 <sup>a</sup>	0.54 ± 0.18 <sup>a</sup>
LOBt	Nil	0.72 ± 0.96 <sup>a</sup>
WOBt	Nil	0.05 ± 0.72 <sup>a</sup>
DORD	3.83 ± 0.33 <sup>a</sup>	5.75 ± 0.84 <sup>b</sup>
AW	43.57 ± 2.47 <sup>a</sup>	78.88 ± 6.11 <sup>b</sup>
THICKNESS	1.59 ± 0.07 <sup>a</sup>	0.81 ± 0.07 <sup>b</sup>
NOPA (no.)	24.10 ± 2.83 <sup>a</sup>	21.75 ± 2.95 <sup>a</sup>
NOB (no.)	11.13 ± 2.64 <sup>a</sup>	2.67 ± 0.99 <sup>b</sup>
NOBt (no.)	Nil	28.04 ± 2.63 <sup>a</sup>

Values with the same superscript are statistically non-significant; Values with different superscripts are statistically significant.

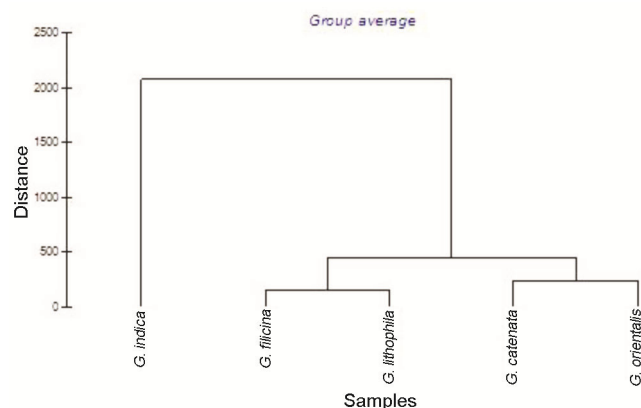


**Figure 3.** Hierarchical cluster analysis showing inter-species affinity.

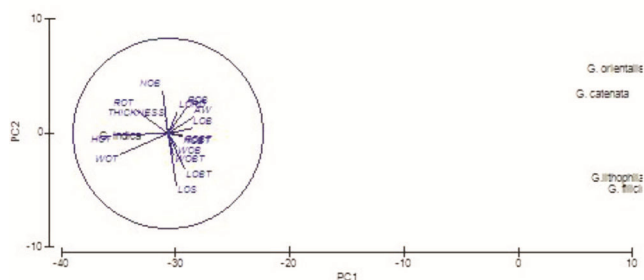


**Figure 4.** PCA plot of *G. filicina*, *G. lithophila*, *G. catenata*, *G. orientalis* and *G. indica* derived from the morphological variables.

generitype<sup>11</sup>, *G. filicina* (Figure 3). Multidimensional scaling analysis revealed 91.04% similarity between *G. orientalis* and *G. catenata* that could be attributable to the morphological similarity between these species (Table 3). The principal component analysis showed a clear distinction between the species based on length and width of the main axis, diameter of rhizoid disk, thickness and number of branches (Figure 4). Samples of *G. orientalis* and *G. catenata* overlapped each other due to high morphological similarity between them.

An inverse relationship was observed between thickness of thallus and length of the primary axis. *G. catenata* showed a relatively thinner of thallus and longer primary axis than *G. orientalis*. Similarly, the number of branches reduces when the thallus grow more. *G. orientalis* had a smaller length and consisted of more number of branches than *G. catenata*. The number and structure of the cortical cell layers were found to be the major distinguishable characters between these species (Table 4).

Around 700 bp of *rbcL* gene was obtained for both species and submitted to GenBank with accession numbers of MT247858–MT247861 (*G. catenata*) and MT247865–MT247867 (*G. orientalis*). Comparison of the present study sequences of *G. catenata* and *G. orientalis* with the NCBI GenBank database showed ~96% similarity (4% divergence) with the reported sequences of *G. catenata* (AB038617: Japan isolate) and *G. orientalis* (HQ829966: China isolate) respectively. The genetic distance value between *G. orientalis* and *G. catenata* was relatively less (0.08%) than the divergence value between *G. catenata* and *G. indica* (Table 5). In the NJ tree, *G. orientalis*, *G. filicina* and *G. lithophila* formed a single clade. *G. catenata* showed a sister relationship to this

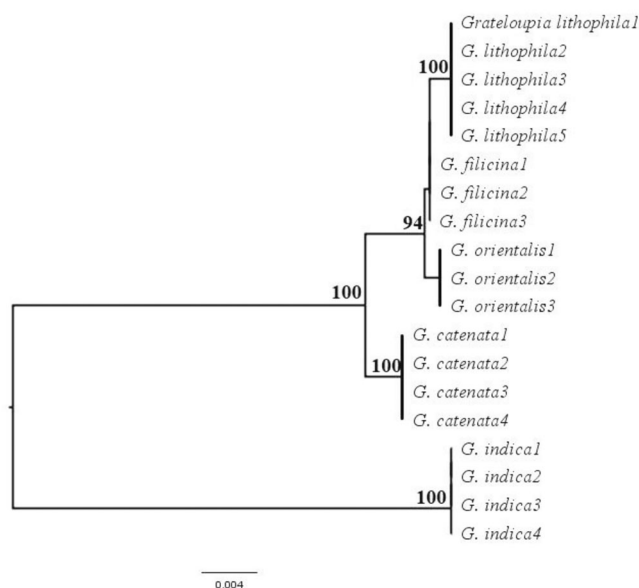


**Figure 5.** Phylogenetic tree (neighbour-joining tree with bootstrap value).

**Table 2.** Correlation matrix of morphological characters of *Grateloupia orientalis* and *Grateloupia catenata*

	HOPA	WOPA	LOB	WOB	LOBt	WOBt	LORD	AW	THICK	NOPA	NOB	NOBt
HOPA	1	0.731	0.552	0.768	0.117	0.172	0.472	0.726	<b>-0.330</b>	<b>-0.003</b>	<b>-0.046</b>	0.697
WOPA	0.731	1	0.336	0.969	0.049	0.222	0.458	0.731	<b>-0.401</b>	<b>-0.022</b>	<b>-0.109</b>	0.746
LOB	0.552	0.336	1	0.351	0.004	<b>-0.129</b>	0.210	0.232	0.061	<b>-0.134</b>	<b>-0.020</b>	0.203
WOB	0.768	0.969	0.351	1	0.017	0.206	0.487	0.737	<b>-0.422</b>	<b>-0.009</b>	<b>-0.113</b>	0.758
LOBt	0.117	0.049	0.004	0.017	1	0.544	0.048	0.111	<b>-0.044</b>	<b>-0.034</b>	0.169	0.046
WOBt	0.172	0.222	<b>-0.129</b>	0.206	0.544	1	0.173	0.203	0.029	0.030	0.209	0.072
LORD	0.472	0.458	0.210	0.487	0.048	0.173	1	0.642	<b>-0.157</b>	0.470	0.325	0.378
AW	0.726	0.731	0.232	0.737	0.111	0.203	0.642	1	<b>-0.353</b>	0.122	<b>-0.055</b>	0.714
THICK	<b>-0.330</b>	<b>-0.401</b>	0.061	<b>-0.422</b>	<b>-0.044</b>	0.029	<b>-0.157</b>	<b>-0.353</b>	1	0.145	0.344	<b>-0.709</b>
NOPA	<b>-0.003</b>	<b>-0.022</b>	<b>-0.134</b>	<b>-0.009</b>	<b>-0.034</b>	0.030	0.470	0.122	0.145	1	0.361	<b>-0.076</b>
NOB	<b>-0.046</b>	<b>-0.109</b>	<b>-0.020</b>	<b>-0.113</b>	0.169	0.209	0.325	<b>-0.055</b>	0.344	0.361	1	<b>-0.300</b>
NOBt	0.697	0.746	0.203	0.758	0.046	0.072	0.378	0.714	<b>-0.709</b>	<b>-0.076</b>	<b>-0.300</b>	1

**Table 3.** Multidimensional scaling analysis

	<i>G. filicina</i>	<i>G. lithophila</i>	<i>G. catenata</i>	<i>G. orientalis</i>	<i>G. indica</i>
<i>G. filicina</i>					
<i>G. lithophila</i>	92.90				
<i>G. catenata</i>	85.16	87.09			
<i>G. orientalis</i>	82.00	81.79	91.04		
<i>G. indica</i>	40.46	41.88	44.27	41.69	

**Table 4.** Comparison of diagnostic features of *G. orientalis* and *G. catenata*

Earlier study	<i>G. orientalis</i>		<i>G. catenata</i>	
	Previous studies <sup>10,12</sup>	Present study	Previous studies <sup>12,14</sup>	Present study
Height of thallus	Up to 16 cm in length	Up to 8.8 cm high	Up to 35 cm high	Up to 9 cm high
Thallus	Bushy, composed of terete to slightly compressed branches bearing irregularly pinnate branchlets	Bushy, erect axes; cylindrical-shaped thallus; terete to slightly compressed branches; branchlets present	Erect axes; terete to compressed branches and tapering towards tapex	Terete to compressed; tapering towards the apex
Texture	Gelatinous and cartilaginous	Mucilaginous and cartilaginous	Slippery and highly gelatinous	Mucilaginous and highly gelatinous
Thickness	0.2–1.5 mm in diameter	Up to 2.3 mm in diameter	Not mentioned	Thickness up to 1.1 mm
Holdfast	Not found	Strong discoid holdfast	Not mentioned	Large discoid holdfast
Reproductive proliferations	Whole thallus, except the basal parts	Common to abundant; present in middle part to apex	Whole thallus	Occasional to abundant; present only at the apex
Cortex cells	6–9 cells	5–6 cells	6–14 cells	5–8 cells
Medullary cells	Hollow in structure	Hollow in structure	Hollow in structure	Hollow in structure
Axillary cell ampullae	Two orders of unbranched filaments which incorporated into a basal fusion cell after diploization of the axillary cell	Present in the secondary medullary filament as an early development stage with continuation of inner cortical cells	–	Entirely absent
Geographical distribution	Taiwan	India (Bay of Bengal)	China, Japan, Korea	India (Bay of Bengal)

clade, with significant bootstrap value (Figure 5). The gene fragment (700 bp of ~1350 bp) studied has low polymorphism to depict phylogenetic relationship that generates less divergence value among the species.

Macro algal groups have extended to different parts of the world by various mechanisms and established in non-native ecosystems. India has a long coast with several major ports that facilitate trade with different nations of the world. Often, along with the ballast water or other

commodities, algae would be transported by ships from their native location to other areas. The presence of major ports like Visakhapatnam and Thoothukudi near sampling sites of the present study could be a possible source for an accidental introduction of *G. orientalis* and *G. catenata* into Indian waters through shipping activity from their native location. The invasive species have relatively high levels of tolerance to ecological perturbations than native species.

**Table 5.** Pairwise genetic divergence value (percentage) among the *Grateloupia* species

Species	Gc	Go	Gf	Gl	Gi
<i>G. catenata</i> (Gc)	0.0 <sup>#</sup>	0.004**	0.009**	0.004**	0.004**
<i>G. orientalis</i> (Go)	0.08*	0.0 <sup>#</sup>	0.001**	0.001**	0.002**
<i>G. filicina</i> (Gf)	0.08*	0.01*	0.0 <sup>#</sup>	0.001**	0.001**
<i>G. lithophila</i> (Gl)	0.09*	0.03*	0.01*	0.0 <sup>#</sup>	0.001**
<i>G. indica</i> (Gi)	6.0*	6.3*	6.1*	6.3*	0.0 <sup>#</sup>

<sup>#</sup>Within species distance values. \*Between species genetic divergence values. \*\*Standard deviation values.

One of the invasive species, *G. turuturu* has been reported to have efficient stress tolerance under adverse environmental conditions and is resistant to hydrogen peroxide, heavy metals, salinity, heat stress and oxidative stress<sup>13</sup>. Accordingly, *G. orientalis* and *G. catenata* may also possess high tolerance capacity to biotic and abiotic stress.

The classical taxonomy of *G. orientalis* and *G. catenata* affirmed that they are different species with some similarities in their morphological features (Table 4). Analysis of morphological data and phylogenetic tree showed that both are closely related species.

In the present study, we characterized *G. orientalis* and *G. catenata* using morphological, anatomical and molecular methods. The study also reports the extended distribution of *G. orientalis* and *G. catenata* in Indian waters and enriches the database of algae from the country. These two species might have entered through shipping activities due to the presence of major ports along the Indian coast. Further studies are required to analyse the population dynamics as well as invasive potential of these species from the Indian coast.

1. Guiry, M. D. and Guiry, G. M., AlgaeBase. World-wide electronic publication. National University of Ireland, Galway, Ireland, 2020; <http://www.algaebase.org> (accessed on 24 March 2020).
2. Miller, K. A., Hughey, J. R. and Gabrielson, P. W., First report of the Japanese species *Grateloupia lanceolata* (Halymeniaceae, Rhodophyta) from California, USA. *Phycol. Res.*, 2009, **57**, 238–241.
3. Montes, M., Rico, J. M., García-Vázquez, E. and Borrell, Y. J., Morphological and molecular methods reveal the Asian alga *Grateloupia imbricata* (Halymeniaceae) occurs on Cantabrian Sea shores (Bay of Biscay). *Phycologia*, 2016, **55**, 365–370.
4. D'Archino, R., Nelson, W. A. and Zuccarello, G. C., Invasive marine red alga introduced to New Zealand waters: first record of *Grateloupia turuturu* (Halymeniaceae, Rhodophyta). *N. Z. J. Mar. Freshw. Res.*, 2007, **41**, 35–42.
5. Oza, R. M. and Zaidi, S. H., *A Revised Checklist of Indian Marine Algae*, CSMCRI, Bhavnagar, 2001, p. 296.
6. Kawaguchi, S., Wang, W. H., Horiguchi, T., Sartoni, G. and Masuda, M., A comparative study of the red algae *Grateloupia filicina* (Halymeniaceae) from the Northwestern Pacific and Mediterranean with the description of *Grateloupia asiatica*, sp. nov. *J. Phycol.*, 2001, **7**, 433–442.
7. Azevedo, C. A. A. D., Cassano, V., Júnior, P. A. H., Batista, M. B. and de Oliveira, M. C., Detecting the non-native *Grateloupia turuturu* (Halymeniales, Rhodophyta) in southern Brazil. *Phycologia*, 2015, **54**, 451–454.

8. Lee, J. I., Kim, H. G., Geraldino, P. J. L., Hwang, I. K. and Boo, S. M., Molecular classification of the genus *Grateloupia* (Halymeniaceae, Rhodophyta) in Korea. *Algae*, 2009, **24**, 231–238.
9. Doyle, J. J., Isolation of plant DNA from fresh tissue. *Focus*, 1990, **12**, 13–15.
10. Lin, S. M., Liang, H. Y. and Hommersand, M. H., Two types of auxiliary cell ampullae in *Grateloupia* (Halymeniaceae, Rhodophyta), including *G. taiwanensis* sp. nov. and *G. orientalis* sp. nov. from taiwan based on *rbcL* gene sequence analysis and cystocarp development. *J. Phycol.*, 2008, **44**, 196–214.
11. Clerck, O. D., Gavio, B., Fredericq, S., Barbara, I. and Coppejans, E., Systematics of *Grateloupia filicina* (Halymeniaceae, Rhodophyta), based on *RbcL* sequence analyses and morphological evidence, including the reinstatement of *G. minima* and the description of *G. capensis* sp. nov. *J. Phycol.*, 2005, **41**, 391–410.
12. Yu, L., Wang, H. and Luan, R., *Grateloupia tenuis* Wang et Luan sp. nov. (Halymeniaceae, Rhodophyta): a new species from South China sea based on morphological observation and *rbcL* gene sequence analysis. *Biomed. Res. Int.*, 2013; <https://doi.org/10.1155/2013/560163>.
13. Liu, F. and Pang, S. J., Stress tolerance and antioxidant enzymatic activities in the metabolisms of the reactive oxygen species in two intertidal red algae *Grateloupia turuturu* and *Palmaria palmata*. *J. Exp. Mar. Biol. Ecol.*, 2010, **382**, 82–87.
14. Wang, H. W., Kawaguchi, S., Horiguchi, T. and Masuda, M., Reinstatement of *Grateloupia catenata* (Rhodophyta, Halymeniaceae) on the basis of morphology and *rbcL* sequences. *Phycologia*, 2000, **39**, 228–237.

ACKNOWLEDGEMENTS. We thank the Director, ICAR-Central Institute of Fisheries Education, Mumbai for providing the necessary facilities and funds to carry out this work. The first author thanks Indian Council of Agricultural Research, New Delhi for JRF fellowship.

Received 20 November 2019; revised accepted 9 July 2020

doi: 10.18520/cs/v119/i5/849-854

## Securing the livelihood of small and marginal farmers by diversifying farming systems

Bussa Bhargavi<sup>1</sup> and Umakanta Behera<sup>2,\*</sup>

<sup>1</sup>Division of Agronomy, Indian Council of Agricultural Research, Central Institute for Cotton Research, Nagpur 440 010, India

<sup>2</sup>College of Agriculture, Central Agricultural University, Kyrdemkulai, Umiam 793 103, India

**Mono-cropping of rice-wheat system in the Indo-Gangetic Plains (IGP) has resulted in natural resource degradation, decline in farm profitability, factor productivity and environmental security. Contrary to mono-cropping, biodiversity is considered as an index to agricultural sustainability. Accordingly, an integrated farming system (IFS) model involving land-based enterprises – crops, dairy, fishery, duckery, poultry, biogas plant and agroforestry was developed in 1 ha area at the ICAR-Indian Agricultural Research**

\*For correspondence. (e-mail: ukb2008@gmail.com)